Data, Range and Adjustment of Affinity Transformations in Photogrammetric Rectifiers

DR. C. A. TRAENKLE,
*Aeronautical Research Laboratory, Wright Field**

ABSTRACT: *Affinity transformations of planar configurations can be produced in projector equipment by applying Scheimpflug's principle of intermediate tilted images. In this paper the deduction of these problems is based on plain geometrical concepts by which the whole system of relations is simplified and clarified considerably.*

The results include the definition of the affinity parameters, their reduction to random azimuth angles and their graphical representation by Mohr's Circle. Proceeding further, appropriate formulae are deduced to compute the setting data for the rectifiers or reproduction projectors. Moreover these relations are simplified for layout formulae to find the transformation range of any given rectifier. Another simplification leads to a separate adjustment procedure by iterative corrections.

All these theoretical relations were checked experimentally by comparing characteristic grid projections to the corresponding and precomputed control charts: they were verified to be in perfect accordance.

1. REVIEW OF PROBLEM

PHOTOGRAMMETRIC rectifiers are built especially for the purpose of trans-projecting aerial photographs, taken at random tilt originally, to the horizontal datum plane, so that they can be mounted as mosaics; it is a transformation of central perspectives. Th. Scheimpflug showed in 1903 that it is possible to produce affinity transformations by additional translations of the tilted photograph in its plane, whereby a square grid may be transformed into an elongated rectangular, or into a shear deformed parallelogram grid.

These possibilities offer interesting mathematical and technical applications. In this paper the relations between the parameters of the affinity transformation and of the rectifier settings will be deduced, correctly based on concepts of simple geometry. The results can be applied in computing the settings of any large affinity transformations within the range of the respective rectifiers. Primarily the common rectifier types with non tiltable lens (Ref. 1) are considered. But the formulae can be easily transferred and extended to any other type of projector or photographic reproduction apparatus.

Affinity deformations may enter the rectifier process also in small amounts, by one sided shrinkage of the photographic film or the control charts. They can be compensated directly by appropriate settings in the rectifier. Simple adjustment rules will be given for this process. This optical mechanical solution represents an alternative approach in determining the instrument settings of affinity transformation by small iterative corrections. It can also be used as an iteration method for any large affinity transformation, avoiding any computation.

* The author acknowledges the encouragement given by Col. A. J. Lingard, Dr. J. E. Clemens and B. B. Johnstone of the Aeronautical Research Laboratory, Wright Field.

Release for publication given by USAF Technical Information & Intelligence Branch, WPAFB.

2. Geometry of Affinity Transformation

Affinity Transformations are systematic displacements of planar point arrays Their properties will be described by simple geometrical concepts, and their characteristics will be defined by special parameters.

2.1 Deformation of Control Cross

Any affinity Transformation may be reduced to an elongation Δd along its principal axis W

$$\Delta d = d\sigma, \tag{1}$$

where d is the distance of the point from the neutral axis V, and σ is the affinity parameter of resultant displacement; if σ is negative, the field undergoes a compression. This relation is applied to the control cross of Figure. 1 which is normally used in the adjustment process of rectifiers (Ref. 2). The control cross is an array of four control points ($A_1A_2B_1B_2$) forming the two diagonals A and B approximately perpendicular to each other and intersecting at about the distance c; the axes system V, W is rotated against A, B by the azimuth angle ω. The array $A_1A_2B_1B_2$ is transformed by Eq. (1) into $A_1'A_2'B_1'B_2'$, whereby the distances d of $A_1B_1 \cdots$ are the components c'', c' of c respectively. To see the relative displacements, the diagonal points of A, for example, have to be put into coincidence again, while the displacements are observed at the probe diagonal B: This operation means that the configuration is rotated by the angle ϵ and reduced by the ratio c_A/c, whereby the points $A_1'A_2'$ move into A_1A_2 and $B_1^rB_1'$ into B_1B_1'' respectively. The reference point B_1^r is set by rotating $\Delta OA_1A_1'$ by 90° into the B-diagonal. Only the displacements of B_1 are further considered, as those of B_2 are of the same amount and antisymmetrical. For small σ, it is vectorially

$$\overline{B_1'B_1''} = \overline{B_1^rB_1} = \overline{c''\sigma},$$

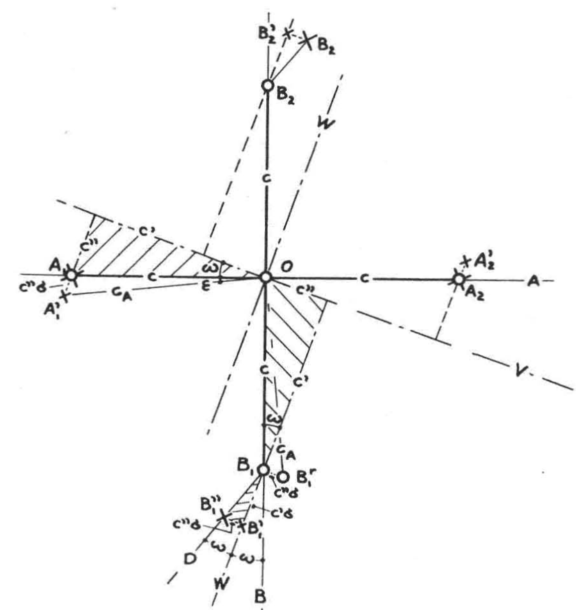

Fig. 1. Transformed check configuration.

and by similar triangles

$$\angle B_1'B_1B_1'' = \omega.$$

This leads to the important relation:

> "The principal affinity axis W is the bisectrix of the D-direction and the B-diagonal."

If the parameter σ is of considerable amount and is taken in one single step, the above statement has to be refined by corrections, as shown in §3.

2.2 MOHR'S CIRCLE

The configuration around Point B_1, Figure 1 is redrawn to a larger scale in Figure 2, to clarify the decomposition of the relative displacement vector B_1B_1'': its amount is $c\sigma \equiv s$ according to similar triangles, and it should be decomposed along the A, B-axes of the control cross as $r \equiv c\rho$, $u \equiv c\mu$ respectively. The parameters of the affinity transformation are defined by ratioing those displacements to $c=1$, as:

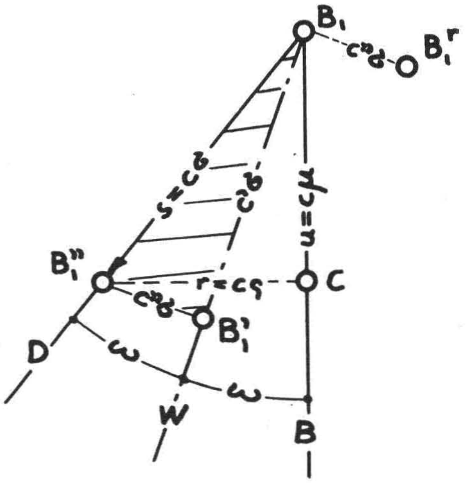

FIG. 2. Displacement components.

$$\sigma \equiv s/c \quad \text{composite parameter,}$$

$$\rho \equiv r/c \quad \text{shear parameter,}$$

$$\mu \equiv \mu/c \quad \text{elongation parameter,}$$

$$\angle B_1''B_1C = 2\omega.$$

Obviously μ, ρ may be interpreted as an elongation and a shear ratio respectively. The configuration of Figure 2 is redrawn in Figure 3 for the parameter values σ, μ, ρ in the

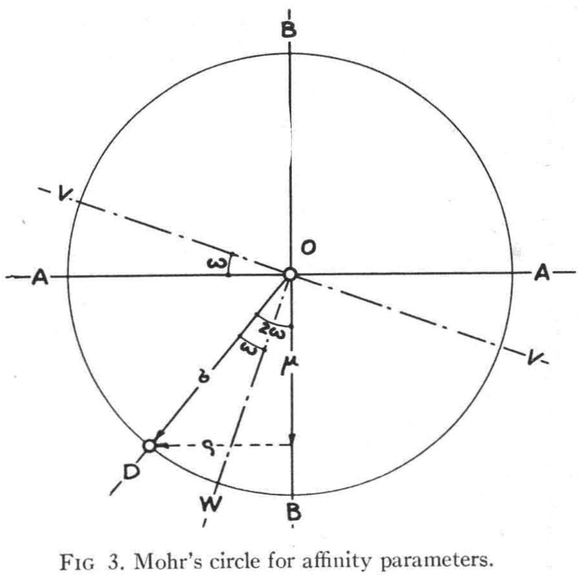

FIG 3. Mohr's circle for affinity parameters.

direction of the corresponding angles. If the principal axes VW are rotated against AB by ω, the resultant parameter $D(\sigma)$ rotates by 2ω and projects the correlated components

$$\mu = \sigma \cos 2\omega, \qquad \rho = \sigma \sin 2\omega$$

on B, A respectively. The arrangement is analogous to Mohr's Circle for the interdependence of the elements of the stress tensor, expressing basically an identical affine relationship.

The above results can be deduced also by analytic means as shown in other papers (Ref. 3), but the geometrical approach as demonstrated here is especially direct.

2.3 REDUCTION OF PARAMETERS TO EASEL AXES

Normally the control cross will have a random azimuth (ω_{BU} in Figure 4) against the easel axes R, U with a resultant vector $\bar{s}\cdot_B$ of affinity displacement (direction D_B, amount s). Now the control cross has to be reduced to $\omega=0$, as the corresponding displacement vector $\bar{s}\cdot_U(D_U)$ has a close relationship to the compensating displacements of the negative carrier. In Figure 4 W is the bisectrix of B, D_B and remains invariant for all ω. According to Mohr's Circle D_B rotates by ω_{BU} into D_U and B into U by the same angle. After that the displacement vector $\bar{s}\cdot_U(D_U)$ is resolved into the components $r\cdot$, $u\cdot$ (Figure 5), by which the negative displacements can be directly determined according to §6.

All configurations so far designed would lie on the projection plane of the

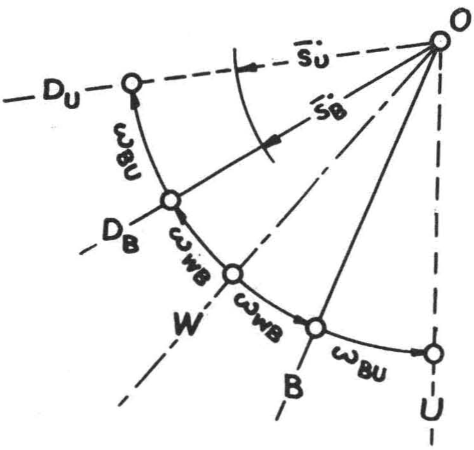

FIG. 4. Axes transition.

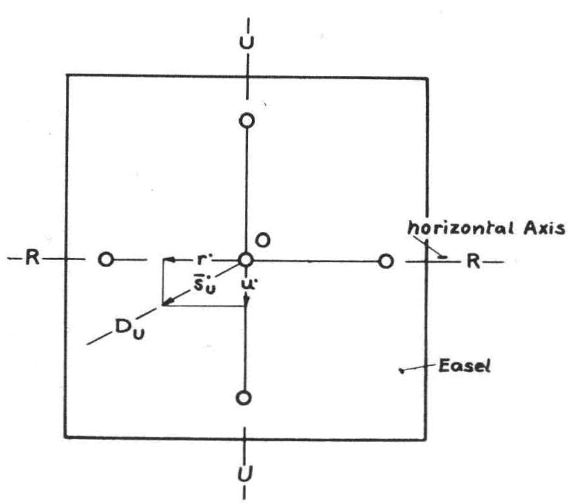

FIG. 5. D_U—reduction to basel axes $R-U$.

projector device. If they have to be distinguished from those on the negative plane, the former will be marked by dot superscripts as in Figure 5.

3. Polar Reduction of Affinity Parameters

The reverse problem is to find the setting data $\omega_*\sigma_*$ of the composite affinity transformation for given component parameters μ^*, ρ^* (Figure 6). The problem is solved in first approximation $\omega^*\sigma^*$ by Mohr's Circle:

$$tg2\omega^* = \rho^*/\mu^*, \qquad \sigma^* = (\rho^{*2} + \mu^{*2})^{1/2}. \tag{2}$$

Now the polar parameters $\omega^*\sigma^*$ have to be reduced to the correct setting values $\omega_*\sigma_*$ if σ is of considerable amount, as mentioned in §2.1.

This reduction has already been prepared in Figure 1: The set polar parameters ω, σ effect a deformation on the control cross, resulting in a relative displacement

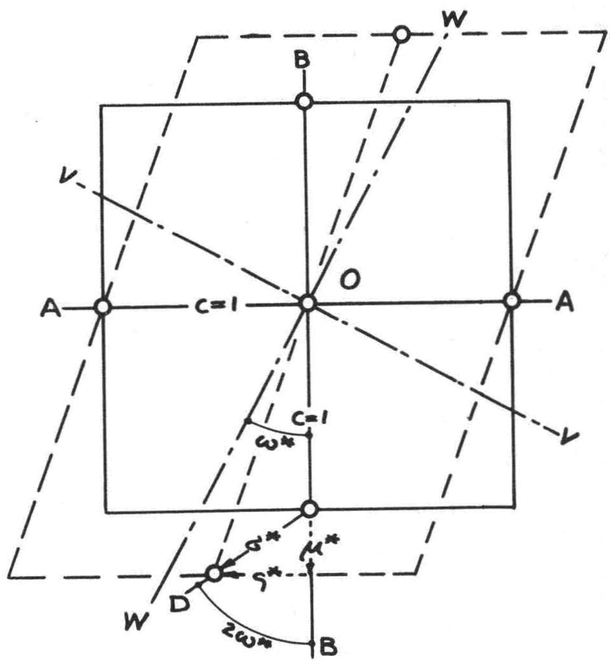

Fig. 6. Composition of affinity components.

placement $\Delta d = B_1{}^r B_1{}''$ of the check point B_1, which has to be referred to the transformed B-axis $OB_1{}^r$ and reduced by the ratio c/c_A. For better clarification and accuracy the B_1-configuration of Figure 1 has been redrawn in Figure 7, whereby the subscript 1 has been omitted and the componential end points B^r, B' of the σ-circle are transferred to the unity circle $c=1$ as O^r, O' respectively. Now the resulting component parameters $\mu'\rho'$ can be found graphically by resolving the vector O^rO' upon the direction OB^r and normal to it, and by considering the scale factors $m = 1/\sigma$, $m' = c_A/\sigma$. It is convenient to interpret the components $\mu'\rho'$ as generated by the vector σ' under the azimuth angle ω'. The relations follow directly from the geometry of Figure 7:

$$\rho = \sigma \sin 2\omega, \qquad \mu = \sigma \cos 2\omega;$$

$$tg\epsilon = \sigma \sin \omega \cos \omega/(1 + \sigma \sin^2 \omega) = (\rho/2)/(1 + \sigma \sin^2 \omega);$$

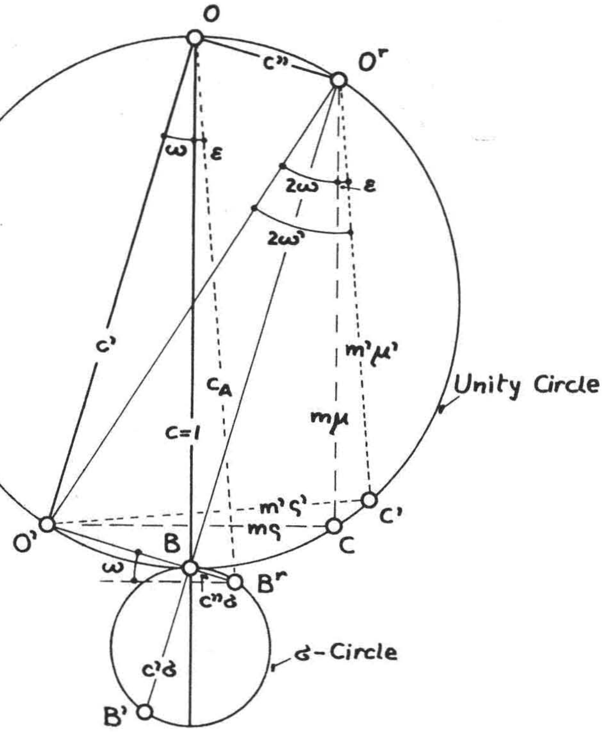

FIG. 7. Polar reduction.

$$C_A{}^2 = (1 + \sigma \sin^2 \omega)^2 + (\rho/2)^2;$$
$$2\omega' = 2\omega + \epsilon, \quad \text{or} \quad \omega' = \omega + \epsilon/2;$$
$$\sigma' = \sigma/c_A;$$
$$\rho' = \sigma' \sin 2\omega', \qquad \mu' = \sigma' \cos 2\omega'.$$

This chain of transcedent equations constitutes the exact relationship between the setting values ω, σ and the resulting transformation components ω', σ', whi ch should be made equal to $\omega^*\sigma^*$ of Eq. (2). These equations cannot be easily rev ersed, but nevertheless they can be solved conveniently by iteration. The first ste p is started with:

$$\omega_1 = \omega^*, \qquad \sigma_1 = \sigma^*.$$

The corrections for the nth step are:

$$\Delta\omega_n = \omega^* - \omega_n', \qquad \Delta\sigma_n = \sigma^* - \sigma_n',$$

and the starting values for the next step:

$$\omega_{n+1} = \omega_n + \Delta\omega_n, \qquad \sigma_{n+1} = \sigma_n + \Delta\sigma.$$

The procedure converges very rapidly to the required setting values

$$\omega \longrightarrow \omega_*, \qquad \sigma \longrightarrow \sigma_*.$$

A numerical example is given in Table 1: the end values are attained already after the 2. step.

TABLE 1
POLAR REDUCTION

Step	ω [°] σ	$\sin\omega$ $\sigma \sin\omega^2$	$\sin 2\omega$ $\cos 2\omega$	q μ	$tg\,\varepsilon$ ε [°]	C_A^2 C_A	ω' [°] σ'	$\Delta\omega$ [°] $\Delta\sigma$
*				0.2000 0.2000			22.50 0.2828	
1	22.50 0.2828	0.3827 0.0414	0.7071 0.7071	0.2000 0.2000	0.0960 5.48	1.0945 1.0462	25.24 0.2703	−2.74 +0.0125
2	19.76 0.2953	0.3381 0.0338	0.6363 0.7713	0.1879 0.2278	0.0909 5.19	1.0776 1.0381	22.36 0.2845	+0.14 −0.0017
3	19.90 0.2936	0.3404 0.0340	0.6401 0.7682	0.1879 0.2255	0.0909 5.19	1.0780 1.0383	22.50 0.2828	0 0

ω_* σ_* ω^* σ^*

The arrangement of Figure 7 can also be used for a rapid graphical solution in connection with the above correction formulae $\Delta\omega_n$ and ΔG_n.—Another graphical solution of this problem by trial and error is described by K. Schwidefsky (Ref. 4).

The above analytical computation is preferable, if higher accuracy is required.

4. RECTIFIER DATA FOR AFFINITY TRANSFORMATION

To set the rectifier for the above determined affinity parameters, it is necessary to compile the respective relations for the rectifier; as to the known details of this theory, it is referred thereby to the handbooks of photogrammetry (Ref. 5).

4.1 PERSPECTIVE TRANSFORMATION

The essential rectifier elements are arranged in Figure 8: The negative plane is transformed to the projection plane as a central projection with the projective center in L standing for a lens of focal distance f_R. The normal lens plane, the negative and the projection plane intersect in one common trace S (Scheimpflug-condition). The magnification ratio n for the optical axis is

$$n = b/a = tg\beta/tg\alpha,$$

and the optical distances a, b are according to the lens formula

$$a = \left(1 + \frac{1}{n}\right) f_R, \qquad b = (1 + n) f_R.$$

The important vanishing points W, V in the negative and projection plane respectively are fixed by the distances h', f', which can be expressed by the triangles of Figure 8

$$f_R = h' \sin\alpha = f' \sin\beta.$$

The transformation formulae for the central projection turn out most simply, if the origins of the coordinate systems x, y and x', y' are put into the vanishing points W, V respectively. The coordinates (x', y') of the projected point M· follow then from the similar triangles of Figure 8:

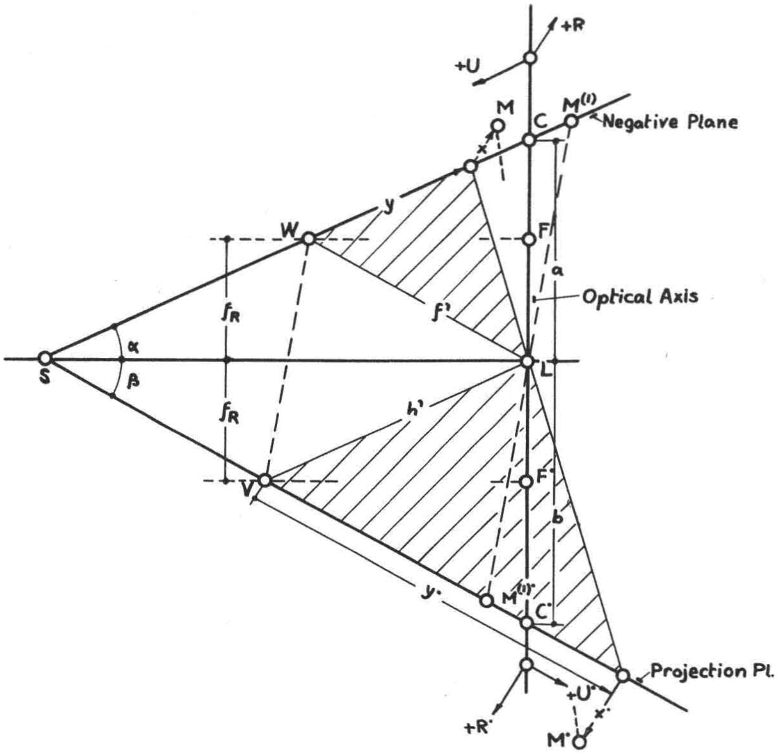

FIG. 8. Perspective transformation.

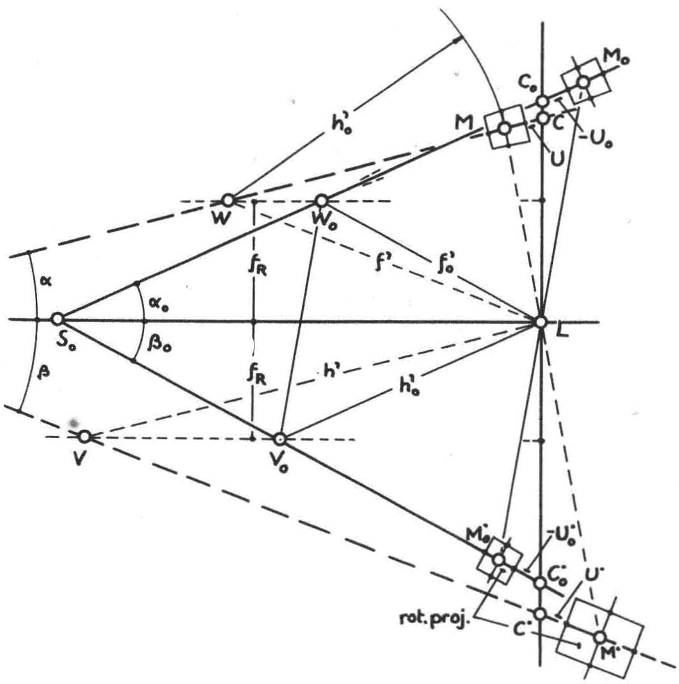

FIG. 9. Transition zero-T-stage.

$$x^{\cdot} = xh'/y, \quad y^{\cdot} = h'f'/y.$$

The local deformations of the transformed field are checked by the magnification ratios m_x, m_y, deduced by differentiation:

$$m_x \equiv \Delta x^{\cdot}/\Delta x = h'/y, \quad m_y \equiv \Delta y^{\cdot}/\Delta y = (-)h'f'/y^2.$$

An important special case, used afterwards, is the unit magnification $m_x = 1$, with:

$$y^{(1)} = h', \quad m_y{}^{(1)} = f'/h'.$$

In this case, it can be seen from Figure 8:

$$M^{(1)}M^{(1)\cdot}//WV.$$

4.2 ZERO STAGE

The affinity transformation is made in subsequent steps. The original square grid is first projected into an intermediate tilted image with set values of tilt angles, displacement U of the negative and m_x. By making $m_x = 1$ the intermediate image is about of the same size as the original; this is practical, as the intermediate image, after being photographically printed, has to be put into the negative carrier (M_0 in Figure 9). Here at first all the setting data for the negative and projection side are reversed. Therefore the intermediate image M_0 is projected back on the projection plane into the original square grid M_0' again, This configuration designated as "Zero Stage" (subscript 0), is used as reference position. Its setting data follow from the geometry of Figure 9; at the same time they are identical with those of the intermediate image after proper interchanging of the designations.
Given Data:

$$f_R, \beta_0. \ U_{0^{\cdot}}, m_{x0} = 1.$$

Computation:

$$\begin{aligned} f_0' &= f_R/\sin \beta_0, \\ tg\alpha_0 &= f_R/(f_0' - U_{0^{\cdot}}) \cos \beta_0, \\ h_0' &= f_R/\sin \alpha_0, \\ U_0 &= f_0' \cos \beta_0/\cos \alpha_0 - h_0'. \end{aligned}$$

4.3 AFFINITY PARAMETERS AND T-STAGE

The general transformation of the original grid is characterized by the affinity parameters μ, ρ (or σ) and by the magnification m_x. Those parameters determine reciprocally the rectifier settings, especially the basic parameters f' and h'. The totality of these parameters and settings constitutes the Transformation-Stage (T-Stage). The equations for these parameters will be deduced from the geometry of Figure 9.

A first requirement of the affinity property is that the side lines of the grid remain parallel, when going from M_0' to M'; this is fulfilled if the vanishing point distance is maintained:

$$WM = W_0M_0 = y_m = h_0' \quad \text{(Vanishing Point Condition)}.$$

The affinity elongation of $M^{\cdot}$ compared to M_0' is characterized by the cross ratio q of the magnifications m_x, m_y, by means of the equations of §4.1:

$$q \equiv m_y/m_x = f'/y = f'/h_0'.$$

Now the ratioed elongated y-side of the grid is by definition $1+\mu$, and it can be also expressed as q/q_0, because the intermediate image is identical in M and M_0:

$$1 + \mu = q/q_0 = f'/f_0', \quad \text{or} \quad f' = (1 + \mu)f_0'. \tag{3}$$

By this equation f' can be computed, if μ is prescribed.

The shear deformation ρ is generated by translating the intermediate image by the amount R in the cross direction (x). The vanishing point W_0, or W, is then displaced by the same amount. The shear of the projected grid lines is determined by this displacement R with reference to L at the distance f_0' if one relates the shear deformation to the original grid length:

$$\rho \equiv r/c = R/f_0'. \tag{4}$$

The affinity parameters have been deduced by the magnification ratios m_x, m_y, which are at first only valid for a small field around the centers M, $M^{\cdot}$. But by the vanishing point condition it is made sure that the transformation is a true affine one in any case for which the affinity parameters are constant over the whole field. Therefore if the parameters are set correctly for the center, they are valid over the whole field.

The magnification m_x follows from the equation of §4.1, by substituting $y_M = h_0'$:

$$m_x = h'/h_0', \quad \text{or} \quad h' = m_x h_0',$$

whereby h' is defined for a given m_x. Likewise it follows by substituting into the transformation formula:

$$y_{M^{\cdot}} = m_x f'.$$

In the case of setting the composite affinity parameter σ in the principal plane U, according to §3, one has to distinguish between the magnification m_x^* of the grid x (or A) axis and the magnification m_x to be set in the projector for its x (or R) axis under the azimuth ω. Their relation follows directly from Figure 7:

$$m_x = m_x^*/c_A.$$

The remaining parameters of the T-stage can now be computed at last by means of the geometrical relations of Figure 9:

$$\begin{aligned}
\sin \alpha &= f_R/h', \\
\sin \beta &= f_R/f', \\
U &= f' \cos \beta/\cos \alpha - h_0', \\
U^{\cdot} &= m_x f' - h' \cos \alpha/\cos \beta.
\end{aligned}$$

A numerical example for the above deductions is given in Table 2 of §7.

There are known also other analytical methods to compute the setting data for affinity transformations (Ref. 6). The above geometrical deductions, while correct for any large range, are however easy to overlook and simple to apply.

5. Transformation Range

By means of the above equations it is possible to compute exactly the parameters and data of any given affinity transformation, and to check afterwards if

TABLE 2

RECTIFIER PARAMETERS, $f_R=138.9$ MM., $c=50$ MM.

Grid No. / Affn. Param.	Stage / m_x	α [°] / β	$\sin\alpha$ / $\sin\beta$	$\cos\alpha$ / $\cos\beta$	$tg\,\alpha$ / $tg\,\beta$	h' [mm] / f'	n / k	U [mm] / U'	R / a
1	0	25.0	0.4226	0.9063	0.4663	328.7	1.3922	−92.6	0
$\mu=0.6$	1	32.99	0.5445	0.8388	0.6492	255.1	—	−100.0	238.7
$\varsigma=0$	T	25.0	0.4226	0.9063	0.4663	328.7	0.7763	+94.8	0
$\omega=0$	1	19.90	0.3403	0.9403	0.3620	408.2	6	—	317.8
	T	12.20	0.2113	0.9774	0.2163	657.4	1.6736	+64.0	0
	2	19.90	0.3403	0.9403	0.3620	408.2	3	—	221.9
2	0	30.0	0.5000	0.8660	0.5774	277.8	1.0	0	0
$\mu=0.2$	1	30.0	0.5000	0.8660	0.5774	277.8	—	0	277.8
$\varsigma=0.2$	T	30.0	0.5000	0.8660	0.5774	277.8	0.7937	+72.2	−55.6
$\omega=0$	1	24.62	0.4166	0.9090	0.4583	333.4	6	—	313.9
	T	14.48	0.2500	0.9682	0.2582	555.6	1.7750	+35.2	−55.6
	2	24.62	0.4166	0.9090	0.4583	333.4	3	—	217.2
3	0	30.0	0.5000	0.8660	0.5774	277.8	1.0	0	0
$\mu=0.2$	1	30.0	0.5000	0.8660	0.5774	277.8	—	0	277.8
$\varsigma=0.2$	T, $m_x^*=1$	31.29	0.5193	0.8545	0.6079	267.5	0.6896	+110.1	0
$\omega=19.9°$	0.9631	22.74	0.3865	0.9222	0.4192	359.4	6	—	340.3
$\sigma=0.2936$	T, $m_x^{**}=2$	15.05	0.2596	0.9657	0.2688	535.1	1.5595	+65.4	0
$c_A=1.0383$	1.9262	22.74	0.3865	0.9222	0.4192	359.4	3	—	228.0

these are lying within the range of the available projection apparatus. For lay-out purposes and planning it is however expedient to have simple, explicit and even approximative formulae by which the principal data and the transformation range covered by the equipment can be overlooked at a glance.

By transposing Eq. (3), it is

$$\mu = (f' - f_0')/f_0.$$

For normal applications the angles α and β are relatively small values ($\lessapprox 30°$), for which the cosine-function is not too far from 1. Therefore it is approximately (Figure 9)

$$f' - f_0' \approx U - U_0,$$

where $U - U_0 = \overline{U}$ denotes the whole available U-range. With

$$f_0 \approx f_R/\beta_0$$

and substituting one obtains

$$\mu = \overline{U}/f_0 \approx \overline{U}\beta_0/f_R, \tag{5}$$

and correspondingly, starting from Eq. (4):

$$\rho = \overline{R}/f_0' \approx \overline{R}\beta_0/f_R. \tag{6}$$

These equations are identical with those given formerly in Ref. 3, Eqs. (31), (32) and deduced there analytically. The above equations show that the affinity parameters are equally dependent on the two factors of the negative displacement ($\overline{U}$ or $\overline{R}$) and of the tilt angle. As a numerical example for the B. & L. Autofocus Rectifier with the given data of

$$f_R \approx 139 \text{ mm.}, \qquad \overline{U} \approx 165 \text{ mm.}, \qquad \overline{R} \approx 180 \text{ mm.}, \qquad \beta_0 \approx 30°,$$

the maximum values of the affinity parameters are approximately

$$\mu_{mx} \approx 0.62, \qquad \rho_{mx} \approx 0.67.$$

These values are very high indeed for one step only. If still higher values are required, the process can be repeated in multiple stages, whereby the subsequent parameters $(1+\mu)$ would be composed by multiplication, and the ρ by addition.

6. Adjustment Procedure by Iterative Corrections

Apart from the exact computation of affinity parameters for large transformations, there are other important applications, where the projected configuration shows only small residual affine deviations from the control grid. Such residual deviations may be encountered for example in aerial photographs to be reduced to a system of control points by rectifier, as in solving resection problems or in making mosaics.

In §2.3 this residual deviation, denoted as the displacement vector $\bar{s}\cdot_B$ of the control cross, is determined by applying first the adjustment rules of perspective transformation of Ref. 3 for example, and is reduced subsequently to the Easel Axes as vector $\bar{s}\cdot_U$ with the components $u\cdot$, $r\cdot$. Now these components can be interpreted as small increments of the affinity parameters

$$\Delta\mu = u\cdot/c\cdot, \qquad \Delta\rho = r\cdot/c\cdot, \qquad c\cdot = m_x c_0,$$

where c_0 is the grid constant of the original square grid. On the other hand there results by differentiation of Eqs. (5), (6):

$$\Delta\mu = \Delta U/f_0', \qquad \Delta\rho = \Delta R/f_0'.$$

By comparison the ratios between the displacements of the negative carrier and the corresponding affinity displacements are

$$\Delta U/u\cdot = f_0'/c\cdot, \qquad \Delta R/r\cdot = f_0'/c\cdot,$$

constituting an identical overcorrection factor k for both the U- and R-component:

$$k = f_0'/c\cdot = f'/c_{u}\cdot = f_0'/m_x c_0, \quad \text{where} \quad c_u\cdot = (1+\mu)c\cdot = c\cdot f'/f_0, \tag{7}$$

by which k can be easily calculated. Incidentally this k-factor is identical with that of the azimuth overcorrection factor of Ref. 2, Eq. (3) for $m_x=1$, going back to identical relations with the vanishing point distance.

Numerical values of k for the example of §7 are compiled in Table 2. Practical adjustments show that for small residual affinity deviations, just one correction step according to Eq. (7) is sufficient to reduce those deviations beyond the threshold value of resolution.

7. Experimental Checks

The above theoretical relations were checked experimentally: A series of test grids were prepared with different affinity parameters; see Figure 10: Grid No. 1 to 3, Form c to be transformed from the original square grids, Form a, via the intermediate tilted images, Form b. The transformations were made by a

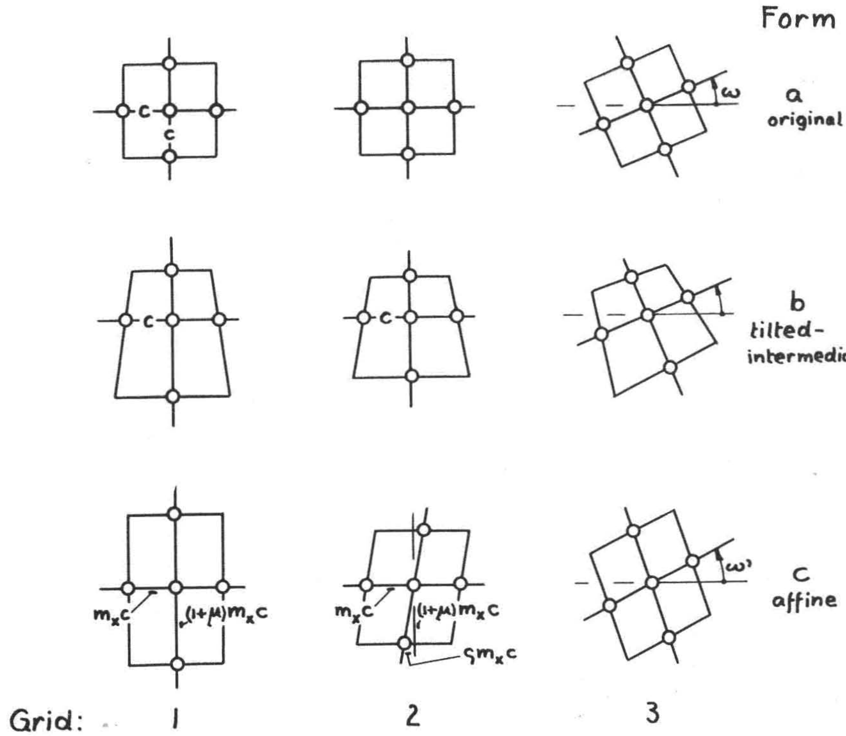

FIG. 10. Grid transformation.

B. & L. Autofocus Rectifier. Its setting data were computed by the equations of § 2, 3 and 4 above, and are compiled in Table 2. The intermediate images were set according to these data, projected from the negative carrier onto the grids, Form *c* on the easel, and checked with respect to coincidence, which turned out to be perfect within the limits of the instrument resolution.

Grid 1 was designed especially to verify the single step range of the μ-affinity parameter, according to Eq. (5): the computed data are definitely confirmed by the experimental results.

Grid 2 gives an example for a general transformation with μ- and ρ-parameters to be simultaneously set. This can be performed very conveniently with rectifiers, where the cross translation of the negative carrier is especially built in.

Grid 3 is identical with Grid 2, but demonstrates how to set the composite affinity parameter σ in the principal plane U, if no R setting is available, as for example in simple reproduction projectors. The preliminary computation for the azimuth setting of the intermediate image is compiled in Table 1, while the computations for the transformation stages are in Table 2. The experiments also verify the perfect coincidence between the preset projection and the control chart.

Finally the Iterative Procedure of §6 was checked. The overcorrection factors k for the above grids were computed according to Eq. (7) and are also compiled in Table 2. Starting from a rough setting of the projection and grid configuration, a perfect coincidence can be quickly adjusted by the above iterative corrections. The convergence was proved to be very rapid, although the factor k is deduced for small angles α, β, but which are in this example rather high.

References

1. For example: B. & L. Autofocus Rectifier, *Zeiss SEG V*, etc.
2. Traenkle, C. A., "Reduction Process of Resection Problems by Photogrammetric Rectifiers," PHOTOGRAMMETRIC ENGINEERING, XXII, 4.
3. Traenkle, C. A., "Affine Bildumformung mittels Entzerrungsgerät (Affinity Transformation by means of Rectifiers)," *Zeitschrift fur Instrumentenkunde*, 64 (1944), 90.
4. Schwidefsky, K., "Uber affine Bildwandlung durch optische Projektion (On Affinity Transformation by Optical Projection)," *Optik Zeitschrift*, 2 (1947), 434.
5. Altenhofen, R. E., "Rectification," MANUAL OF PHOTOGRAMMETRY, IX, 1952.
6. See e.g. Ref. 4 and Ref. 2.

news 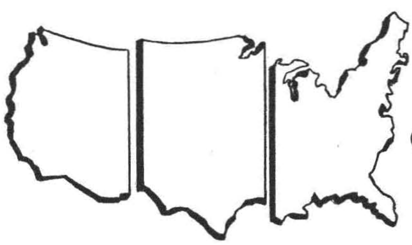 OF THE SECTIONS

ST. LOUIS SECTION

The Membership Committee of the St. Louis Section has been set up to aid Society Members in any of the following ways:

1. Select committee members from Society members in good standing. (Chairman)
2. Provide information to interest prospective members in the value of membership.
3. Develop programs and techniques for obtaining members in accord with policies of President and Board of Direction.
4. Plan and program membership campaigns in accordance with policies and objectives of President and Board of Direction.
4. Execute a yearly program for maintaining current membership and obtaining new members.
6. Support the National Society in specific membership program and related matters.
7. Provide periodic and annual reports of status and activities as required. (Chairman)
8. Represent the local Section in membership matters. (Chairman)
9. Submit recommendations for the good of the Society.

Any problems or questions related to the above functions can be referred to any of the following committee members:

PHILIP RAHALL, *Chairman*
LOUIS J. REED, *Director Member*

Last summer Professor Young, University of Maine, attended a forest soils meeting in Ontario, Canada. At that time W. G. E. Brown, Soils Specialist, Forest Research Division, Forestry Branch, Department of Northern Affairs and National Resources, Ottawa, Canada demonstrated with airphotos the technique that he has developed for doing P.I. from a soils standpoint on airphotos. Dys Burger of the Ontario Dept. of Lands and Forest did P.I. on over 3,000 square miles from a soils standpoint, during a three months period in the winter of '54–'55 using these techniques.

Prof. Young has received a reprint of "Roads and Land" by W. G. E. Brown which was originally published in *Timber of Canada* in February, 1956. Very likely many U. S. citizens do not see this publication. It is believed that his agency has an ample supply of reprints for anybody interested.